www.sciencemag.org/content/347/6217/83/suppl/DC1

Supplementary Materials for

Lysosomal signaling molecules regulate longevity in *Caenorhabditis elegans*

Andrew Folick, Holly Doebbler Oakley, Yong Yu, Eric H. Armstrong, Manju Kumari, Lucas Sanor, David D. Moore, Eric A. Ortlund, Rudolf Zechner, Meng C. Wang*

*Corresponding author. E-mail: wmeng@bcm.edu

Published 2 January 2015, *Science* **347**, 83 (2014)
DOI: 10.1126/science.1258857

This PDF file includes

Materials and Methods

Caenorhabditis elegans strains and generation of transgenic lines

Wild type (N2) and BX165 (*nhr-80(tm1011)III)* were obtained from the *Caenorhabditis* Genetics Center*; nhr-49(nr2041)* was a gift from A. Antebi; VS17 (*hjIs9[ges-1p::glo-1::gfp]*) was a gift from H.Y. Mak*; nape-1(tm3860)* and *lipl-4(tm4417)* were obtained from the National Bioresource Project, Japan; *lbp-8(rax1)* was generated by EMS mutagenesis and backcrossed 10 times into the N2 genetic background.

For the generation of transgenic strains, gonads of young adult N2 worms were injected with DNA mixture using the standard method. For the generation of integrated strains, late L4 stage strains containing extrachromosomal arrays were exposed to 4500 rads of gamma irradiation in 5.9 minutes, and integrated strains were backcrossed to N2 at least 5 times. We generated and used the following transgenic strains: *raxIs3[ges-1p::lipl-4::sl2gfp], raxEx32[lbp-8p::lbp-8::sl2gfp], raxIs4[lbp-8p::lbp-8::sl2gfp], raxEx20[ges-1p::lipl-4::3xFLAG::sl2rfp], raxEx31[lbp-8p::lbp-8::3xFLAG::sl2rfp], raxEx48[ges-1p::lbp-8::mcherry], raxEx55[ges-1p::lipl-4(no SP)::3xFLAG::sl2gfp]* (deletion of 21 N-terminal residues)*, raxEx51[ges-1p::lbp-8(no NLS)::3xFLAG::sl2gfp]* (deletion of 37 N-terminal residues).

Characterization of lipase activity

The worm lysate was prepared using a modified version of the previously described method (*19*). For each sample, approximately 20,000 synchronous Day 2 adult worms were collected using M9 buffer, washed three times in M9 buffer, washed twice in Extraction buffer A (10 mM sodium acetate pH 5.0, 0.1 mM DTT and 1 mM PMSF), and pelleted in a minimal volume of buffer A. The worm pellet was homogenized in 200µL of Extraction Buffer B (10 mM sodium acetate pH 5.0, 0.1 mM DTT, 1 mM PMSF, 1x proteinase inhibitor and 1% v/v Triton X-100), and sonicated 6 times for 1 minute on ice with low energy. After centrifugation at maximum speed for 10 min at 4°C, the supernatant homogenate was collected in a new tube and flash frozen in liquid nitrogen. For the determination of triacylglycerol hydrolase activity, the reaction mixture was prepared by mixing the worm lysate (40 µg protein) and 100 µl of substrate in a total volume of 200 µl. The substrate was prepared by emulsifying 33 nmol triolein/assay (glycerol tri[9,10(n)-^{3}H] oleate 40,000cpm/nmol) and 45 µM phosphatidylcholine:phosphatidylinositol (3:1) by sonication in 100 mM potassium phosphate buffer (pH 7.4) and 2% fatty acid free BSA. Each reaction was incubated at 37^{o}C for 60 min (*20*). The reaction was terminated by addition of 3.25 ml of methanol:chloroform:heptane (10:9:7 v/v/v) and 1 ml of potassium carbonate, 0.1 M boric acid, pH 10.5. After vigorous vortex, samples were centrifuged at 800 g for 15 min. Free fatty acid liberated by lipase activity in the worm lysate was determined by measuring radioactivity in 1 ml of the upper aqueous phase by liquid scintillation counting.

Fluorescent microscopy

Day 1 adult worms were mounted on 2% agarose pads containing 0.5% NaN_3 as anesthetic on glass microscope slides. Fluorescent images were taken using an Axioplan 2 microscope (Zeiss) connected to an Axioplan MrC camera (Zeiss) for fig. S5A.

Immunofluorescence staining

Performed at room temperature unless otherwise indicated. Young adult worms were dissected in EBT (10% 10X Egg Buffer, 0.1% Tween-20 in ddH_20), and fixed by adding Fixative Solution (10% Egg Buffer, 7.4% formaldehyde in ddH_20). A cover slip was applied and liquid was removed to adhere worm tissue to Superfrost Plus slides (VWR). The slides were frozen on an aluminum block and stored at -80°C overnight. The following day, the cover slip removed and the slides were immediately placed in -20°C methanol for post-fixation then washed 3 times with PBST (PBS with 0.1% Tween-20). They were blocked with 0.5% BSA in PBST in a humid chamber, and washed with PBST. The primary antibody (see below) was applied for 2 hours in a humid chamber followed by 3 times wash with PBST. Secondary antibodies were applied for 2 hours in a dark humid chamber followed by 3 times wash with PBST. The slides were mounted using Vectashield mounting medium with DAPI (Vector Laboratories). Imaging was performed using a FluoView FV1000 confocal microscope (Olympus).

Primary antibodies: anti-FLAG monoclonal mouse IgG (Sigma, F3165) 1:200 in PBST, anti-GFP rabbit polyclonal IgG (Santa Cruz Biotech, SC-8334) 1:200 in PBST, anti-LMP-1 monoclonal mouse IgG (DSHB, University of Iowa) 1:200 in PBST. Secondary antibodies: Alexafluor 488 goat anti-rabbit IgG (Invitrogen, A-11008) 1:500 in PBST, Alexafluor 555 donkey anti-mouse IgG (Invitrogen, A-31570) 1:500 in PBST.

Lysotracker staining

LysoTracker Green DND-26 (Molecular Probes) was diluted in ddH_2O to 100μM, and 200 μL were added to each 6 cm standard NGM plate (containing 12mL of agar) seeded with OP50. The plates were kept in the dark for 24 hours to allow the lysotracker solution to diffuse evenly throughout the plate. 10~20 worms were added to each plate at the L4 stage and kept in the dark for 2 days at 20°C before imaging with a confocal microscope.

Subcellular fractionation and Western blot

Mixed-stage worms were washed once in M9 and 3x in 25 mM HEPES. A 50 μL pellet of worms collected in nuclear isolation buffer (NIB, 10 mM KCl, 1.5 mM MgCl2, 1 mM EDTA, 1 mM EGTA, 1 mM DTT, 0.1 mM PMSF, 250 mM sucrose, 25 mM HEPES, ph 7.5) in a 1.5 ml centrifuge tube. Pellet was ground with plastic pestle and 300 μL NIB was added. Ground worms were transferred to a Dounce homogenizer for 15 strokes on ice. Homogenized sample was centrifuged at 250g for 2 minutes. Supernatant transferred and centrifuged 750g for 10 minutes. Pellet was kept as nuclear fraction and washed 2x in NIB. Supernatant was kept as cytoplasmic fraction and purified by 2x

centrifugation at 750g for 10 minutes. Gel eletrophoresis and transfer to a PDVF membrane were performed. After blocking, primary antibodies were incubated for 1 hour at RT (in PBST with 5% BSA): anti-FLAG monoclonal mouse IgG (Sigma, F3165) 1:2000, anti-LMP-1 monoclonal mouse IgG (DSHB, University of Iowa) 1:400, anti-Histone H3 polyclonal rabbit (Abcam, ab1791) 1:2000, anti-GFP polyclonal rabbit IgG (Santa Cruz Biotech, SC-8334) 1:2000. After 3x washing in PBST, secondary antibodies were incubated for 1 hour at RT: HRP goat anti-rabbit IgG 1:4000, HRP donkey anti-mouse IgG (Santa Cruz Biotechnology) 1:4000. After 3x washing in PBST, membranes were treated with Amersham western blotting detection reagents prior to development.

Metabolite profiling

Metabolomic analysis was performed by Metabolon, Inc. (Durham, N.C.) using six samples each of N2 and *lipl-4 Tg* worms. For each sample, 200,000 age-synchronized worms were grown on *E. coli* OP50 NGM plates and collected as young adults. The worms were washed three times in M9 buffer and returned to empty NGM plates for 30 minutes for gut clearance. Using fluorescently labeled *E. coli*, we found that 30 minutes was the minimum time required for complete clearance of bacteria from the intestine (data not shown). Following intestinal clearance, worms were washed twice more in M9 buffer, pelleted in a minimal volume of M9 and flash frozen in liquid nitrogen. The details of the metabolite profiling platform have been described previously (*21*). Briefly, proprietary recovery standards were added to each sample prior to extraction, and the samples were extracted using the automated MicroLab STAR system (Hamilton Company). The extracted samples were divided equally and prepared for analyses by GC/MS or LC/MS. The LC/MS analysis was based on an Acquity UPLC (Waters Corporation) and a LTQ-FT mass spectrometer with a linear ion-trap (LIT) front end and a Fourier transform ion cyclotron resonance (FT-ICR) back end (Thermo Fisher Scientific Inc.). Two independent injections were performed: one using acidic position ion optimized conditions (water/methanol and 0.1% formic acid) and one using basic negative ion optimized conditions (water/methanol and 65 mM ammonium bicarbonate). The GC/MS analysis was performed using the Trace DSQ fast-scanning single-quadropole mass spectrometer using electron impact ionization (Thermo Fisher Scientific Inc.). For both platforms, metabolites were identified by comparison of chromatographic properties and mass spectra to a reference library of >1000 commercially available purified standard compounds. 352 named compounds were identified in this study. Statistical analysis was performed using Welch's two-sample *t*-test to identify compounds that differed significantly between wild type and *lipl-4 Tg* groups.

Lipid feeding

Age synchronized worms were grown on *E. coli* OP50 NGM plates to the L4 stage. arachidonic acid, ω-3 arachidonic acid, dihomo-γ-linolenic acid, oleoylethanolamide (OEA) or KDS-5104 (Cayman Chemical) was dissolved in ethanol and diluted into M9 buffer to a final concentration of 100 μM and 0.4% ethanol. 300 μL of each mixture was added to 12 mL of worm agar plates with bacterial food, and dried in less than ten

minutes in a laminar flow hood. Worms were collected at 3 hours and RNA extraction and quantitative RT-PCR was performed as described below.

For lifespan experiments, KDS-5104 was dissolved in ethanolamine and diluted into BDR buffer (100 mM, 5.74 mM K_2HPO_4, 44 mM KH_2PO4) to a final concentration of 0, 1, 10, or 100 μM KDS-5104 and 0.4% ethanolamine. 200 μL of each mixture was added to standard 6 cm NGM plates with OP50 bacterial food and allowed to dry at room temperature. Worms were transferred to freshly prepared plates daily, and lifespan was scored as described below.

Lifespan assays

Worms were age-synchronized by bleach-based egg isolation followed by starvation in M9 buffer at the L1 stage for at least 24 hours. For all experiments, every genotype and condition was performed in parallel. Synchronized L1 worms were grown to the first day of adulthood, and Day 0 of the lifespan was determined by the onset of egg-laying. During adulthood, worms were transferred to new plates every two days. 80-100 animals were assayed for each condition/genotype with 30-40 animals per 6 cm plate. Death was indicated by total cessation of movement in response to mechanical stimulation. Statistical analyses were performed with SPSS software (IBM Software) using Kaplan-Meier survival analysis and the log-rank test. For integrated transgenic strains, the strain was backcrossed to *N2* at least five times prior to lifespan analysis (as indicated in Table S1).

For RNAi-based experiments, RNAi clones from the libraries generated in the laboratories of Dr. Julie Ahringer and Dr. Marc Vidal were used. All clones were verified by sequencing. We generated an *lbp-8* RNAi clone by targeting the whole coding region of the gene. Age-synchronized worms were grown on HT115 bacteria transformed with empty L4440 vector until Day 1 of adulthood. 80-100 worms per treatment group were transferred to dsRNA expressing clones or L4440 control. For non-RNAi lifespan experiments, worm were grown their entire lives on *E. coli* OP50 NGM plates (as indicated in Table S1).

Quantitative RT-PCR

Total RNA was isolated from at least 1000 age-synchronized young adult worms using Trizol extraction with column purification (Qiagen). Synthesis of cDNA was performed using the SuperScript III First-Strand Synthesis System (Invitrogen). Quantitative PCR was performed using Kapa SYBR fast PCR kit (Kapa Biosystems) in an Eppendorf Realplex 4 PCR machine (Eppendorf). Values were normalized to *rpl-32* as an internal control. *rpl-32* amounts were stable and consistent with *cdc-42, ama-1,* and *pmp-3* for all strains described (fig. S16). All data shown represent three biologically independent samples. Statistical analysis was performed using the paired two-sample *t*-test for pairwise comparisons and two-way ANOVA to test for interactions of multiple variables.

Competitive Flourescence-based binding assay

LBP-8 was subcloned into pGEX-KG-a plasmid containing the gene encoding glutathione S-transferase (GST). GST-fused to LBP-8 (GST-LBP-8) was induced with 0.5 mM isopropyl-1-thio-b-D-galactopyranoside (IPTG) for 24 hours at 16°C, expressed in *E. coli* BL21 (DE3) strain (Stratagene) and purified using glutathione-Sepharose 4B beads (GE). Quantification of ligand binding was conducted via competition of the probe 1-anilinonaphthalene-8-sulfonic acid (1,8-ANS), a small molecule whose fluorescence increases drastically when surrounded by a hydrophobic environment and which has been shown to bind an array of intracellular lipid binding proteins (iLBPs) with varying affinity (*22*). In brief, binding of 1,8-ANS was carried out in PBS (137 mM NaCl, 2.7 mM KCl, 10 mM Na_2HPO_4, 2 mM KH_2PO_4, pH=7.4) in the presence of 250 nM GST-LBP-8 and increasing amounts of fluorescent probe (0-40 μM), which was added using 50X ethanol stocks so that final ethanol concentration remained at 2% for all wells. Blank measurements containing 1,8-ANS only were subtracted from each probe concentration tested, and the resulting fluorescent values were normalized prior to determination of the binding constant, K_D. Competition assays were then carried out in the same buffer system using a constant concentration of 250 nM protein and 800 nM 1,8-ANS, with ligand added via 50X ethanol stocks to maintain an ethanol concentration of 2%. Blanks containing probe and ligand only were subtracted from each ligand concentration tested, and fluorescence values normalized before calculation of a ligand's K_i. Data were collected after one hour's time at 25°C on a BioTek Synergy plate reader using an excitation filter of 380/20nm and an emission filter of 460/40nm, and processed in GraphPad Prism 5. All curves are the average of three independent experiments.

NHR binding assay using intrinsic Tryptophan fluorescence

NHR-49 and the ligand binding domain (LBD) fragment of NHR-80 are subcloned into pGEX-KG-a plasmid containing the gene encoding glutathione S-transferase (GST). *Escherichia coli* BL21 (DE3) strain (Stratagene) was cultured in 2XYTmedium and induced for overexpression of GST-NHR-49 and GST-NHR-80LBD by the addition of 1mM IPTG for 2 hours at 23°C. The GST fusion proteins were purified using glutathione–Sepharose beads (GE). For binding assays, 400μL of the GST fusion proteins (~1μg/μL) were added into 10 x 2 mm quartz cuvettes. Fluorescence measurement of the GST fusion proteins was performed in the Cary Eclipse Fluorescence Spectrophotometer (Aligent) with increasing concentration (0~200μM) of OEA (Cayman, 25mM stock in ethanol). The GST fusion proteins were excited at 280 nm and fluorescence emission intensity was monitored for 1 nm intervals at a scan rate of 600 nm/min between 290 nm and 450 nm. The excitation and emission slits are 5nm. The fluorescence emission intensity decreases at 320 nm were calculated and plotted against OEA concentration. Data was fit to a standard binding curve using Prism 5.

Differential Protease Sensitivity Assay

nhr-49a and *nhr-80b* were subcloned into pT7CFE1-Chis for *in vitro translation*. Translation was performed using the TnT Quick Coupled Transcription/Translation System (Promega) with ^{35}S-Methionine labeling. KDS-5104 (10 μM) or vehicle control

(ethanol) was added to the translation reaction and incubated 30 min at 30°C. α-Chymotrypsin (12.5-200 μg/ml, Sigma-Aldrich) was added to the mixture and incubated for 10 min at room temperature. Reaction was stopped with Laemmli Sample Buffer (BioRad). After gel electrophoresis, gel was fixed, treated with Amersham Amplify Fluorographic Reagent (GE Healthcare), dried under vacuum, and exposed at -70°C.

Primers

acs-2 FWD TTCGACCGGATGAGCCAGTAAACA
acs-2 REV GTTGTTGTTCAGCCCGAAATGGGT
lbp-8 FWD AATTGCTCCGGATGAGCGATCCTA
lbp-8 REV TCTCTACGACAAATGACGCTCCCA
lbp-8 Exon 2 FWD GATGAGCGATCCTACAACACTT
lbp-8 Exon 2 REV AACAGAGCTGTGGTGGTTT
rpl-32 FWD AGGGAATTGATAACCGTGTCCGCA
rpl-32 REV TGTAGGACTGCATGAGGAGCATGT
cdc-42 FWD GCCGACAGTCTTCGACAATTA
cdc-42 REV CTTCCTGTCCAGCAGTATCAAA
ama-1 FWD ACGAGTCCGCAGTACAGT
ama-1 REV GAATCCGCGTGGAGATGTT
pmp-3 FWD CAGCTTCTCGACGGTGTTAAA
pmp-3 REV CAGCTCTTCGTGAAGTTCCATA

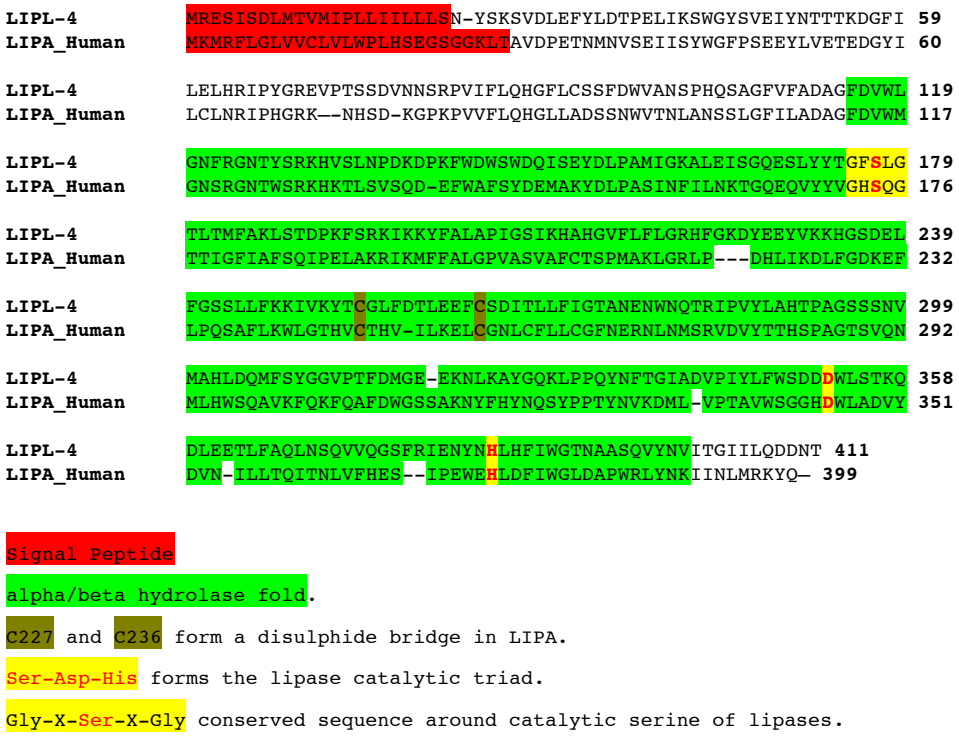

Fig. S1. Sequence alignment of *C. elegans* LIPL-4 and human LIPA.

Sequence alignment between *C. elegans* LIPL-4 and human LIPA highlights the conserved regions critical for the lipase activity.

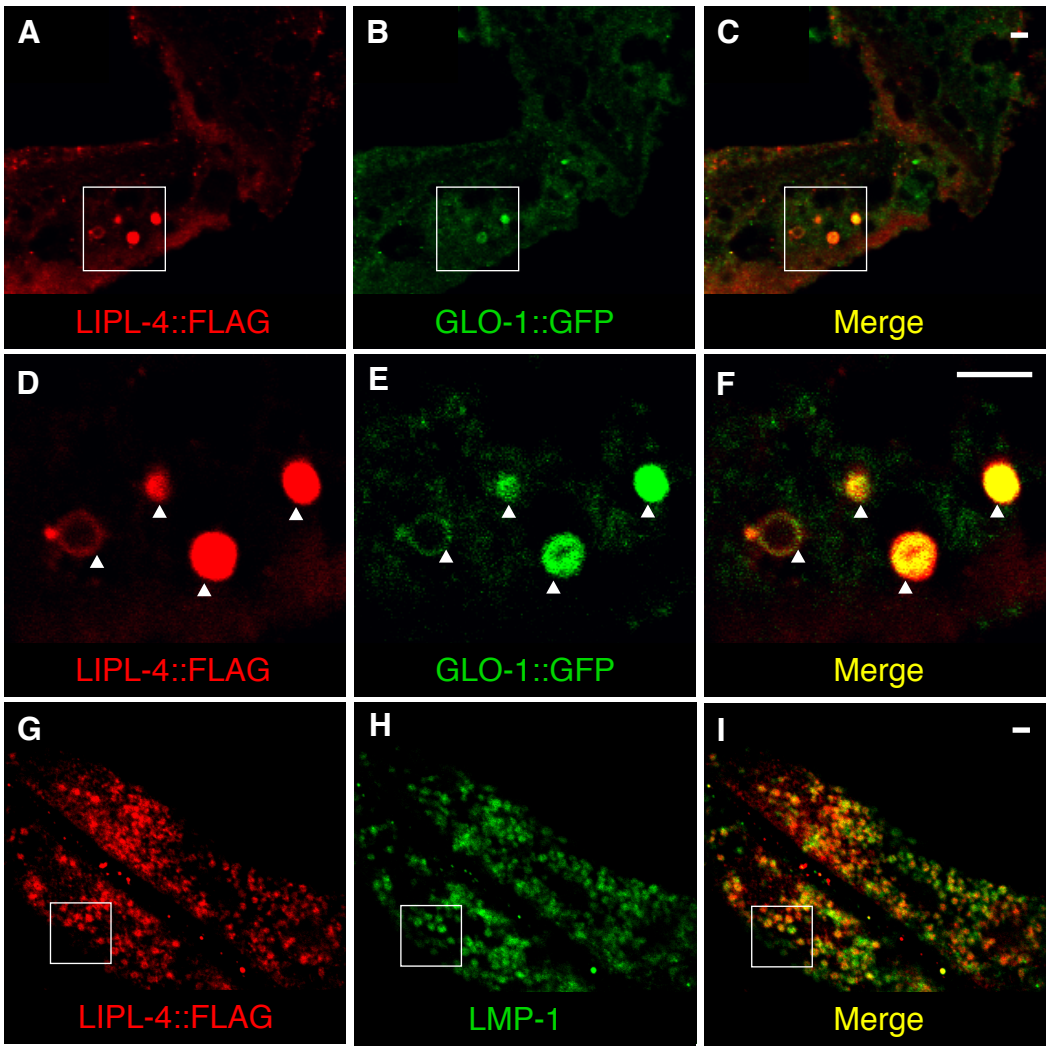

Fig. S2. Intestinal lysosomal localization of LIPL-4.

(A–F) Young adult worms—*raxEx20[ges-1p::lipl-4::3xFLAG]; hjIs9[ges-1p::glo-1::gfp]* expressing both LIPL-4::3xFLAG and GLO-1::GFP fusion proteins—were stained with anti-FLAG (A and D) and anti-GFP (B and E) antibodies. LIPL-4 is co-localized with GLO-1, a protein marker of intestinal lysosome (*23*) (C and F). Scale bar = 10 μm.
(G–I) Young adult worms—*raxEx20[ges-1p::lipl-4::3xFLAG]* expressing LIPL-4::3xFLAG fusion proteins—were stained with anti-FLAG (G) and anti-LMP-1 (H) antibodies. (I) LIPL-4 is co-localized with LMP-1. Enlarged images are shown in Fig. 1B–D. Scale bar = 10 μm.

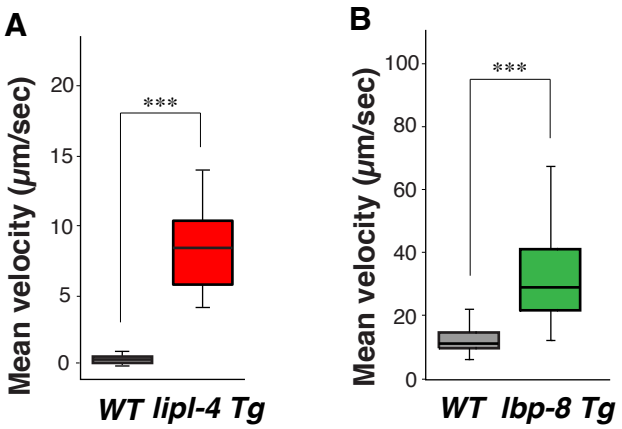

Fig. S3. Constitutive expression of *lipl-4* and *lbp-8* delay age-related decline of physical activity.

(A) Mean locomotion velocity is increased by 10-fold in *lipl-4 Tg* worms compared to WT at age 20 days. ***p<0.001, Student's t-test.
(B) Mean locomotion velocity is increased by 2-fold in *lbp-8 Tg* worms compared to WT at age 15 days. ***p<0.0001, Student's t-test.

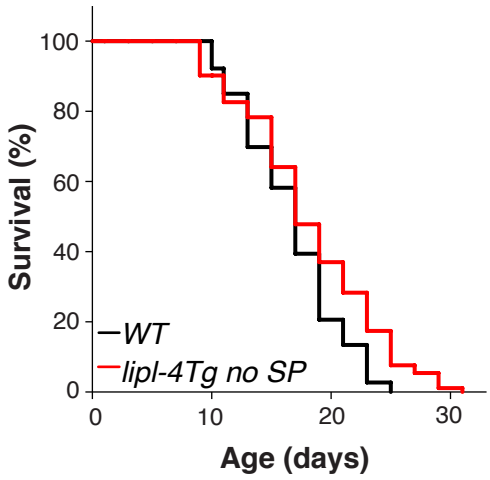

Fig. S4. Lysosomal activity of *C. elegans* LIPL-4 is required for longevity.

Constitutive expression of LIPL-4 without the signal peptide (*lipl-4 Tg no SP, raxEx55[ges-1p::lipl-4(no SP)::3xFLAG::sl2gfp]*), which is not targeted to the lysosome, does not significantly affect lifespan, when compared to WT.

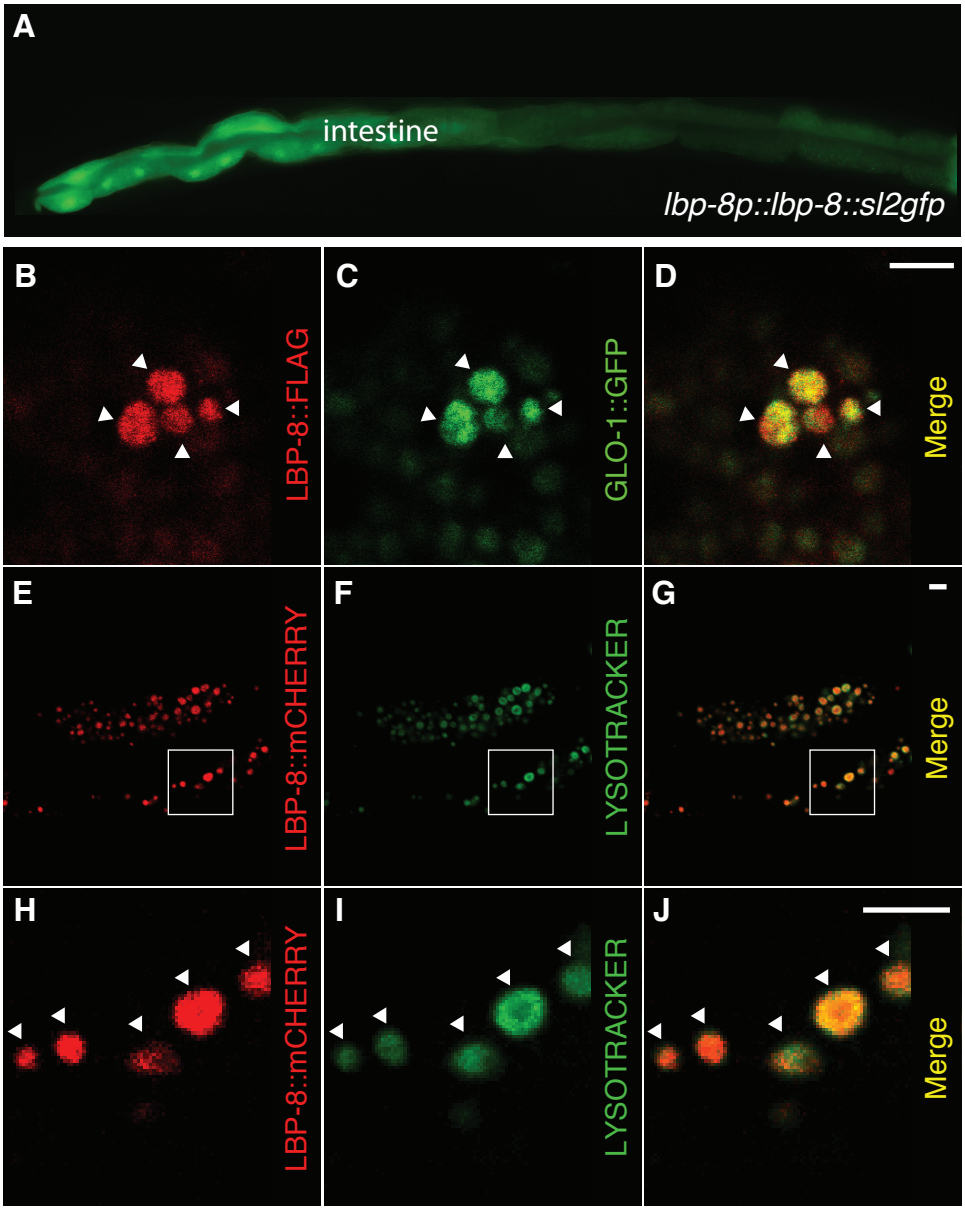

Fig. S5. Intestinal expression and lysosomal localization of *lbp-8*.

(A) An *lbp-8* GFP reporter (*raxEx32[lbp-8p::lbp-8::sl2gfp])* reveals expression of *lbp-8* in intestinal cells in well-fed wild-type worms.
(B-D) Young adult worms— *raxEx31[lbp-8p::lbp-8::3xFLAG];hjIs9[ges-1p::glo-1::gfp]* expressing LBP-8::3xFLAG and GLO-1::GFP fusion proteins—were stained with anti-FLAG (B) and anti-GFP (C). (D) LBP-8 co-localizes with GLO-1, a protein marker of intestinal lysosomes (*24*).
(E-J) Young adult worms—*raxEx48[ges-1p::lbp-8::mcherry]* expressing LBP-8::mCHERRY fusion proteins—were stained with LysoTracker Green. Enlarged images are shown in (H–J).

Lysosomes identified by white arrowheads. Scale bar =10 μm.

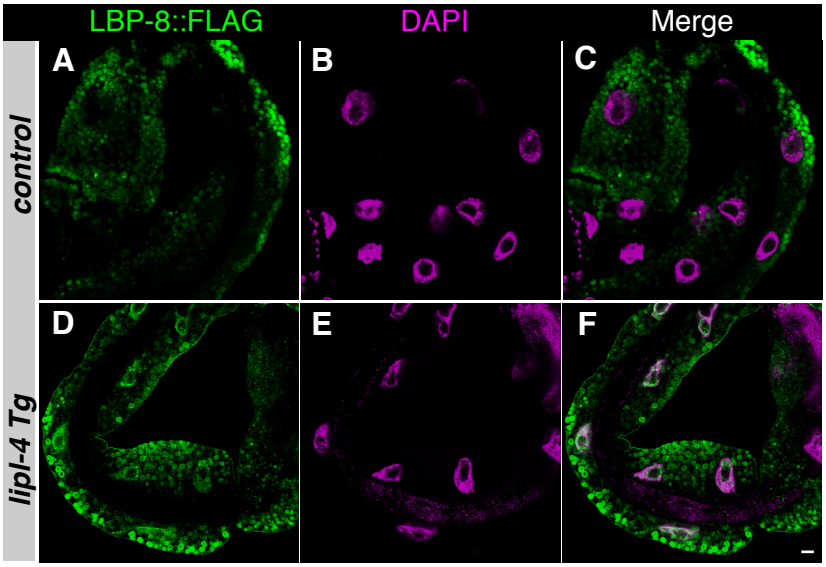

G

LBP-8

MVSMKEFIGRWKLVHSENFEEYLKEIGVGLLIRKAASLTSPTLEIKLDGD 50
TWHFNQYSTFKNNKLAFKIREKFVEIAPDERSYNTLVTFENGKFISHQDK 100
IKENHHSSVFTTWLENGKLLQTYQSGSVICRREFVKE 137

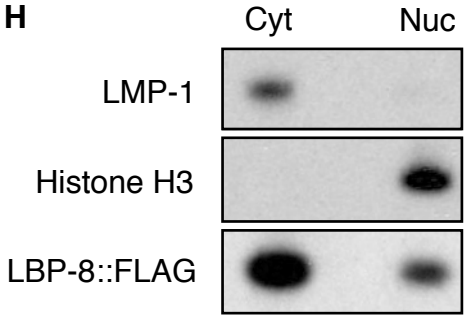

Fig. S6. Nuclear localization of LBP-8.

(A-F) Adult worms expressing LBP-8::3xFLAG were stained with anti-FLAG (A and D) and 4',6-diamidino-2-phenylindole (DAPI; B and E). LBP-8 nuclear localization increases in *lipl-4 Tg* (F) versus control worms (C). Scale bar =10 μm.
(G) Predicted nuclear localization signal in LBP-8. LBP-8 contains a predicted nuclear localization sequence (NLS), highlighted in red at the N-terminus, with a score of 5.3. Prediction of the NLS was performed using cNLS Mapper software (http://nls-mapper.iab.keio.ac.jp/cgibin/NLS_Mapper_form.cgi). An NLS with a score of 5 to 6 predicts protein localization in both the nucleus and the cytoplasm.
(H) Western blots of both nuclear and cytoplasmic fractions of young adult worms, *raxIs3[ges-1p::lipl-4::sl2GFP];raxEx31[lbp-8p::lbp-8::3xFLAG]*. The lysosomal proteins LMP-1 and histone H3 were used as cytoplasmic and nuclear markers, respectively. LBP-8::3xFLAG fusion proteins were detected in both fractions.

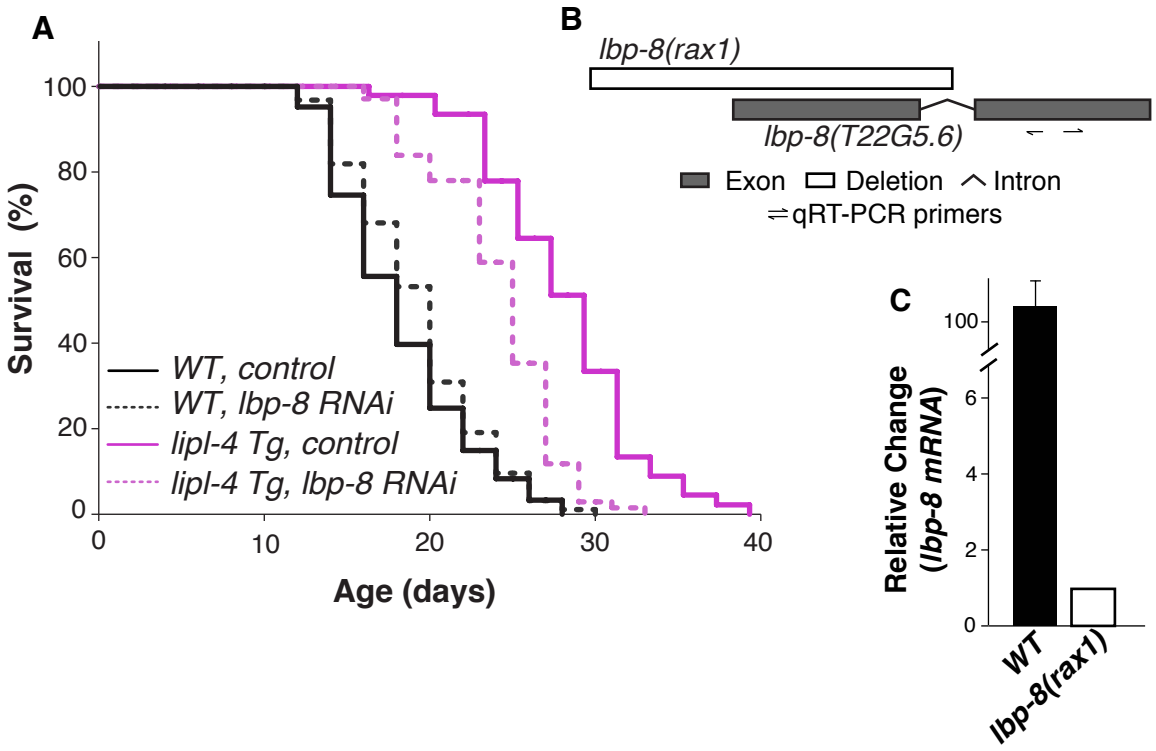

Fig. S7. Requirement of LBP-8 for *lipl-4*-mediated lifespan extension.

(A) Adult-only inactivation of *lbp-8* by RNAi feeding reduces lifespan extension of *lipl-4 Tg* by 51%, $p<0.0001$. RNAi knockdown of *lbp-8* does not alter wild type lifespan, $p>0.5$, Log-rank test.
(B) The *lbp-8(rax1)* deletion encompasses the entire first exon and transcriptional start site.
(C) Using primer sets targeting the second exon, levels of mRNA detection are decreased by >100-fold. Error bars represent S.D.

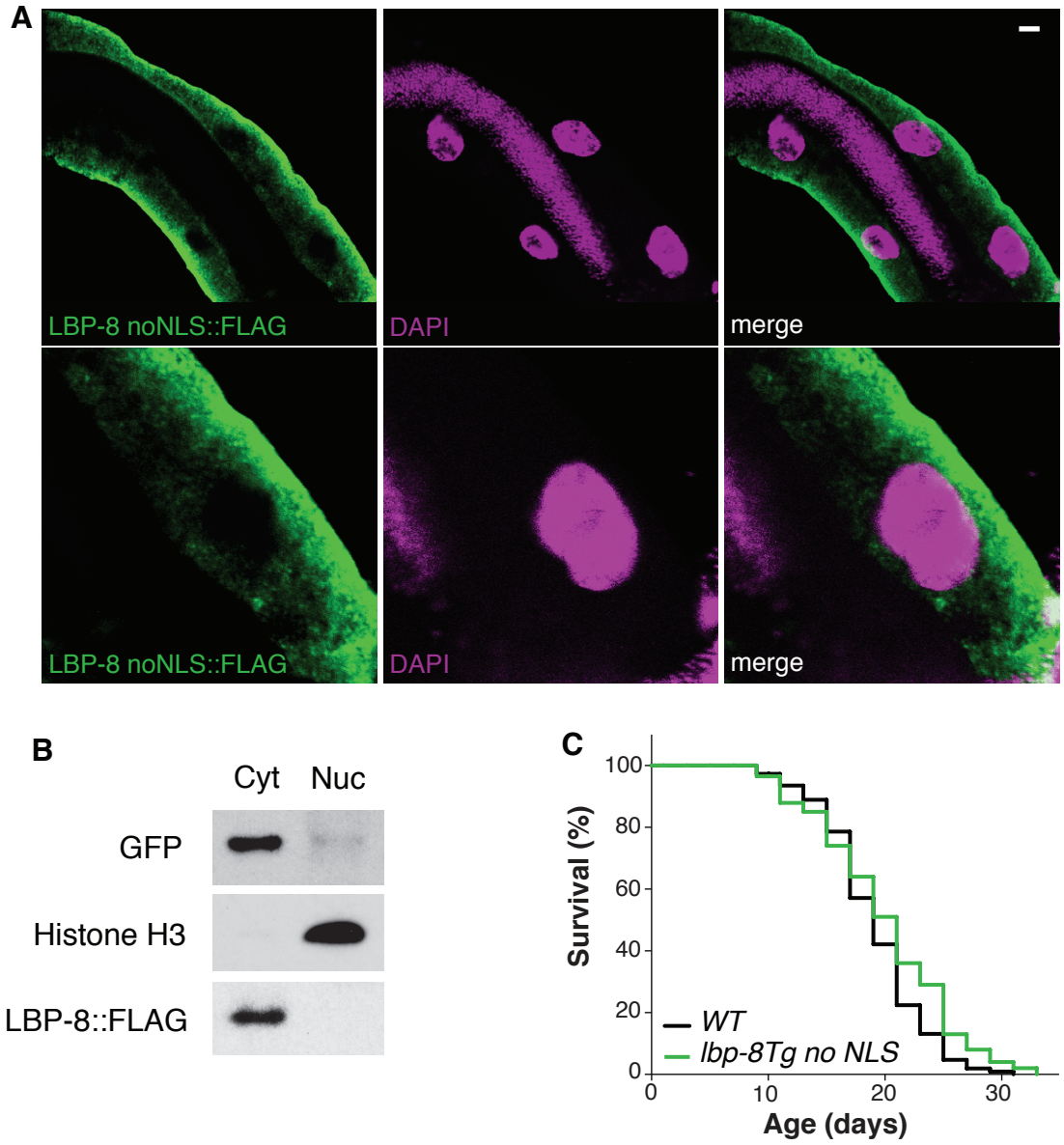

Fig. S8. Nuclear localization of *C. elegans* LBP-8 is required for longevity.

(A) Transgenic worms *lbp-8 Tg no NLS* (*raxEx51[lbp-8p::lbp-8(no NLS)::3xFLAG::sl2gfp]),* expressing 3xFLAG fused LBP-8 proteins lacking NLS, were stained with the anti-FLAG antibody (green). LBP-8 lacking NLS does not localize into the nucleus (DAPI, purple). Scale bar = 10 μm.
(B) Western blots of both nuclear and cytoplasmic fractions of *lbp-8 Tg no NLS* worms. GFP and Histone H3 are used as cytoplasmic and nuclear markers, respectively. LBP-8(no NLS)::3xFLAG fusion proteins were only detected in the cytosplasmic fraction.
(C) Mean lifespan is not significantly different between *lbp-8 Tg no NLS* and WT worms, $p<0.05$, Log-rank-test.

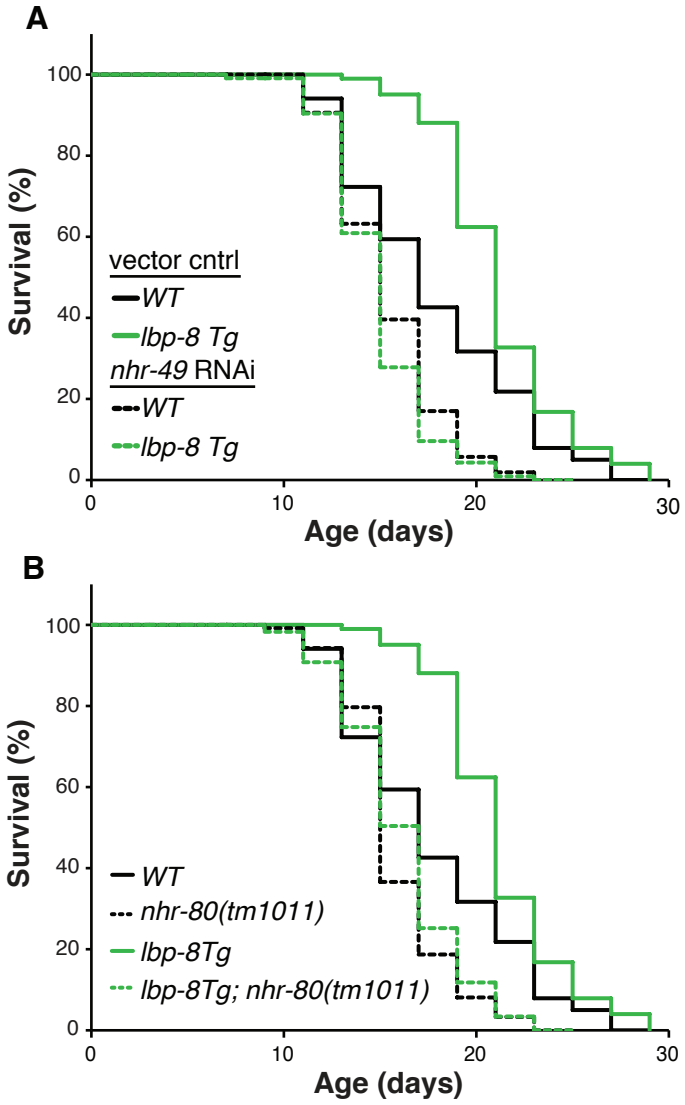

Fig. S9. Requirement of NHR-49 and NHR-80 for *lbp-8*-mediated lifespan extension.

Mean lifespan was not significantly changed in *lbp-8 Tg* worms with RNAi-inactivation of *nhr-49* during adulthood (A) or with the *nhr-80(tm1011)* loss-of-function mutation (B), $p>0.05$, Log-rank test.

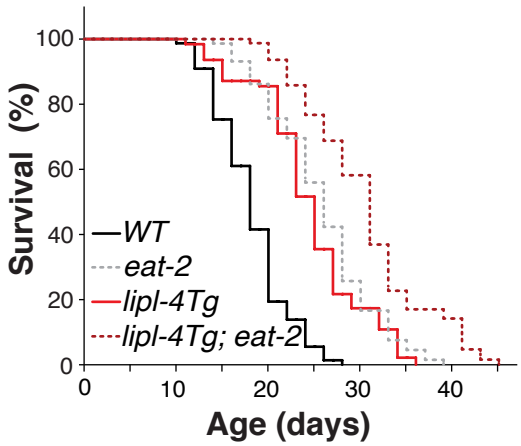

Fig. S10. LIPL-4-mediate longevity acts independent of dietary restriction.

The *eat-2(ad1116)* mutant is a genetic model of dietary restriction in *C. elegans* and lives 42% longer than wild type worms, $p<0.0001$. Constitutive expression of *lipl-4 (lipl-4 Tg)* further enhances the lifespan extension in the *eat-2(ad116)* mutant, $p<0.0001$, Log-rank test.

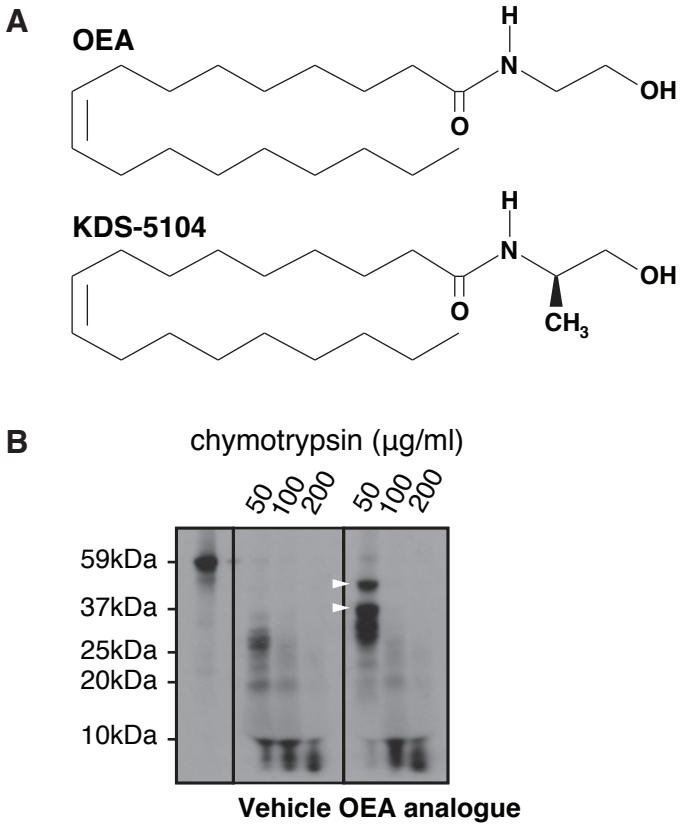

Fig. S11. Binding of OEA analogue,KDS-5104 to NHR80.

(A) Chemical Structures of OEA and KDS-5104. KDS-5104 is a non-hydrolysable analogue of OEA with an additional methyl group and is resistant to degradation by fatty acid amide hydrolase.
(B) 35^{S}-methionine–labeled NHR-80 was treated with increasing concentrations of chymotrypsin (50–200 μg/ml). Fragments of 45 kDa and 35 kDa (arrowheads) were protected from digestion by OEA analogue (10 μM).

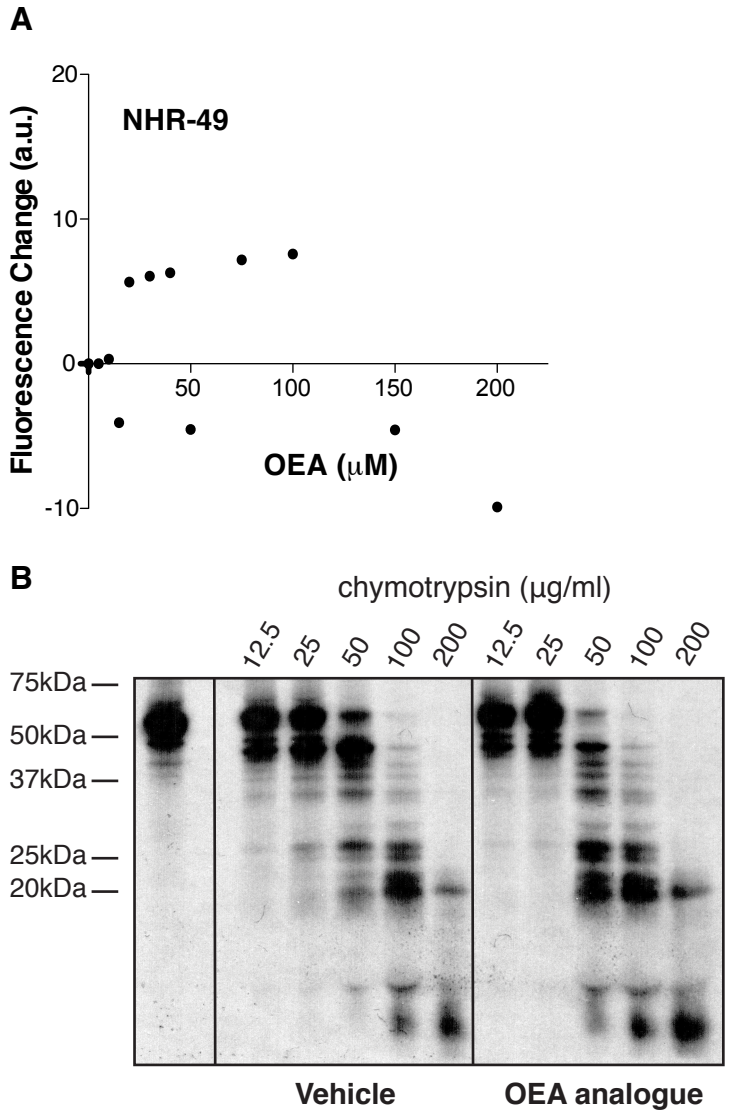

Fig. S12. No direct binding between NHR-49 and OEA or its analogue.

(A) Intrinsic fluorescence changes in the GST-NHR-49 fusion proteins were measured with the increasing concentration of OEA (0-200μM). There was no dose-dependent changes in the fluorescence intensity.

(B) 35^{S}-methionine–labeled NHR-49 was treated with increasing concentrations of chymotrypsin (12.5-200 μg/ml). No protection from chymotrypsin digestion was detected in the presence of OEA analogue (10 μM).

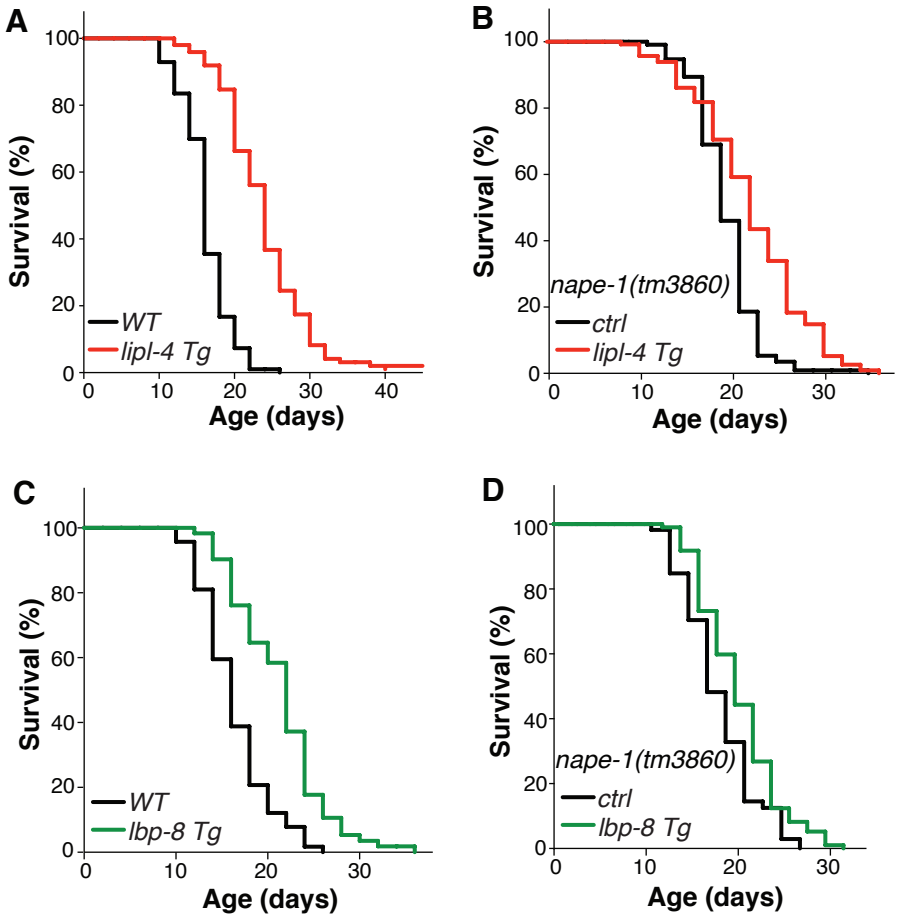

Fig. S13. Requirement of NAPE-1 for *lipl-4*-and *lbp-8*-mediated lifespan extension.

(A and B) The *nape-1(tm3860)* deletion reduces the mean lifespan extension of *lipl-4 Tg* worms from 47.5% (A) to 18.9% (B), $p<0.001$, Log-rank-test.
(C and D) The *nape-1(tm3860)* deletion decreases the mean lifespan extension of *lbp-8 Tg* worms from 30.4% (C) to 18.2% (D), $p<0.001$, Log-rank test.

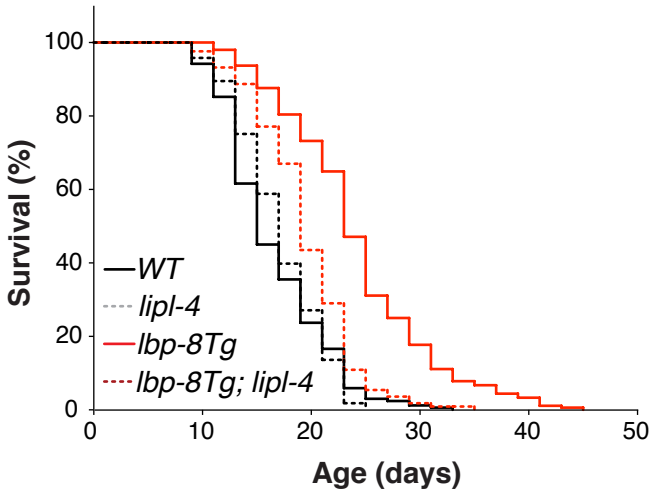

Fig. S14. *lipl-4* is required for *lbp-8*-mediated longevity.

The loss-of-function mutation *lipl-4(tm4417)* reduced the lifespan extension of *lbp-8 Tg* by 68%, $p<0.0001$. *lipl-4(tm4417)* did not affect lifespan in a WT background, $p>0.5$, Log-rank test.

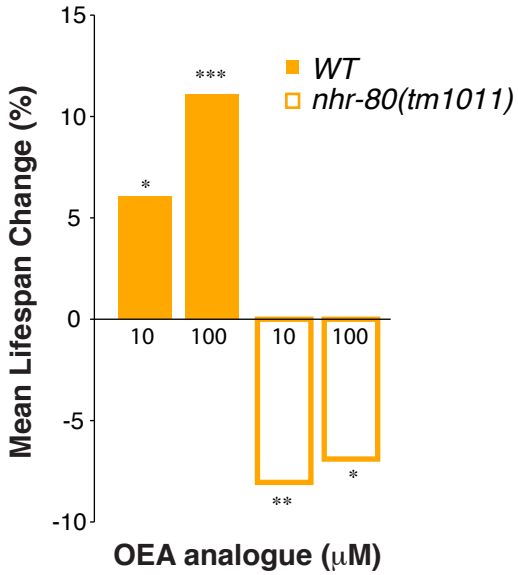

Fig. S15. Requirement of NHR-80 for OEA to promote longevity.

Supplementation of OEA analogue was sufficient to prolong lifespan in WT animals, but decreased lifespan in the *nhr-80(tm1011)* mutants. **p*<0.05, ***p*<0.01, ****p*<0.005, Log-rank test.

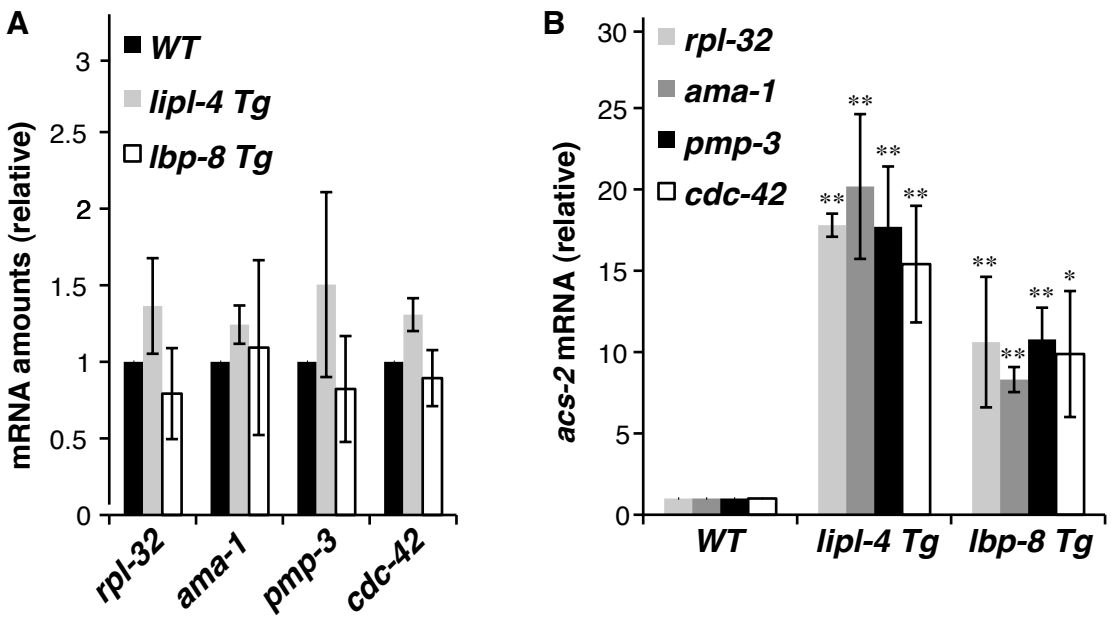

Fig. S16. qRT-PCR results with different housekeeping genes.

The levels of four different housekeeping genes—*ama-1, pmp-3, cdc-42, and rpl-32*—were quantified using qRT-PCR in WT, *lipl-4 Tg* and *lbp-8 Tg* worms . No significant differences were observed between WT and the transgenic worms (A). qRT-PCR quantification of *acs-2* expression, using different housekeeping genes as internal controls, provided similar results (B). **p*<0.05, ***p*<0.01, Student's *t*-test. Error bars respresent S.D.

Table S1. Summary of lifespan analyses.

genotype	*treatment*	*mean lifespan*	*std error*	*p-value*	*n*	*censor*	*backcross*
N2	OP50	17.33	0.42		62	1	
lipl-4 Tg	OP50	26.94	0.52	<0.001	65	16	6x
N2	OP50	18.13	0.30		146	28	
lbp-8(rax1)	OP50	18.68	0.38	0.087	119	29	10x
*lipl-4 Tg**	OP50	24.91	0.48		132	28	10x
lipl-4 Tg; lbp-8(rax-1)*	OP50	22.46	0.50	<0.001	127	36	10x
N2	L4440	18.33	0.52		63	1	
N2	*lbp-8* RNAi	19.28	0.42	0.209	94	0	
lipl-4 Tg	L4440	27.84	0.68		49	4	10x
lipl-4 Tg	*lbp-8* RNAi	24.17	0.46	<0.001	75	7	10x
N2	L4440	18.64	0.42		78	3	
N2	*lbp-8* RNAi	19.98	0.52	0.023	76	1	
lipl-4 Tg	L4440	26.94	0.52		65	16	10x
lipl-4 Tg	*lbp-8* RNAi	24.88	0.44	0.005	74	5	10x
N2	OP50	16.81	0.37		116	32	
non-Tg sibling	OP50	16.70	0.39		117	5	
lipl-4 Tg no SP	OP50	18.20	0.59	0.003	115	23	
non-Tg sibling	OP50	19.01	0.42		121	14	
lbp-8 Tg no NLS	OP50	20.00	0.57	0.022	125	24	
N2	OP50	16.50	0.61		50	22	
non-Tg sibling	OP50	18.22	0.96		50	24	
*lbp-8 Tg**	OP50	21.63	0.79	0.023	50	25	
N2	OP50	17.69	0.46		90	18	
lbp-8 Tg	OP50	23.00	0.49	<0.001	90	28	5x
N2	L4440	15.88	0.40		121	11	
N2	*nhr-49* RNAi	13.11	0.25	<0.001	92	7	
lipl-4 Tg	L4440	20.87	0.54		100	13	10x
lipl-4 Tg	*nhr-49* RNAi	12.81	0.26	<0.001	74	9	10x
N2	L4440	17.11	0.51		92	8	
N2	*nhr-49* RNAi	14.41	0.27	<0.001	88	5	
lipl-4 Tg	L4440	23.08	0.50		93	17	10x
lipl-4 Tg	*nhr-49* RNAi	14.29	0.23	<0.001	94	8	10x
N2	OP50	17.97	0.92		93	7	
nhr-80(tm1011)	OP50	17.45	1.05	0.473	71	19	
lipl-4 Tg	OP50	26.36	0.86		90	10	10x
lipl-4 Tg; nhr-80(tm1011)	OP50	18.31	0.38	<0.001	93	7	10x
N2	L4440	17.69	0.44		112	11	
N2	*nhr-49* RNAi	15.36	0.27	<0.001	117	11	
lbp-8 Tg	L4440	21.12	0.32		121	20	8x
lbp-8 Tg	*nhr-49* RNAi	14.84	0.24	<0.001	118	3	8x
nhr-80(tm1011)	L4440	15.80	0.24		126	3	
lbp-8 Tg; nhr-80(tm1011)	L4440	16.09	0.29	0.298	122	3	8x
N2	OP50	16.16	0.33		120	24	
lipl-4 Tg	OP50	24.11	0.68	<0.001	119	21	10x

nape-1(tm3860)	OP50	18.59	0.32		120	7	
lipl-4 Tg; nape-1(tm3860)	OP50	22.11	0.55	<0.001	120	5	10x
N2	OP50	16.35	0.35		120	4	
lbp-8 Tg	OP50	21.31	0.46	<0.001	125	12	8x
nape-1(tm3860)	OP50	17.29	0.38		120	16	
lbp-8 Tg; nape-1(tm3860)	OP50	20.43	0.44	<0.001	116	19	8x
N2	0 μM KDS	13.27	0.48		121	37	
N2	1 μM KDS	13.71	0.32	0.549	123	31	
N2	10 μM KDS	14.80	0.40	0.141	120	38	
N2	100 μM KDS	15.32	0.83	0.025	107	40	
lipl-4 Tg	0 μM KDS	18.38	0.64		113	42	
lipl-4 Tg	10 μM KDS	18.89	1.01	0.622	122	45	
lipl-4 Tg	100 μM KDS	18.82	0.83	0.144	121	77	
lbp-8 Tg	0 μM KDS	25.43	1.10		122	15	
lbp-8 Tg	10 μM KDS	26.22	0.94	0.377	123	43	
lbp-8 Tg	100 μM KDS	25.03	1.02	0.430	119	39	
N2	0 μM KDS	17.61	0.31		125	20	
N2	10 μM KDS	18.67	0.36	0.010	137	32	
N2	100 μM KDS	19.57	0.49	<0.001	133	38	
nhr-80(tm1011)	0 μM KDS	11.80	0.35		134	31	
nhr-80(tm1011)	10 μM KDS	10.85	0.31	0.007	133	54	
nhr-80(tm1011)	100 μM KDS	10.99	0.31	0.036	131	46	

lipl-4 Tg = raxIs3[ges-1p::lipl-4::sl2gfp]
lipl-4 Tg = raxEx21[ges-1p::lipl-4::3XFLAG::sl2rfp]*
lipl-4 Tg no SP = raxEx55[ges-1p::lipl-4(no LLS)::sl2gfp]
lbp-8 Tg no NLS = raxEx51[ges-1p::lbp-8(no NLS)::sl2gfp]
lbp-8 Tg = raxIs4[lbp-8p::lbp-8::sl2gfp]
lbp-8 Tg = raxEx32[lbp-8p::lbp-8::sl2gfp]*
KDS = KDS-5104, OEA analogue (dissolved in ethanolamine)
p-value by Log-rank test (note: comparison is to nearest above condition without listed *p-value*).

Table S2. Metabolite levels significantly altered in *lipl-4 Tg*.

Biochemical Name	*Platform*	*Fold Change*	*p-value*	*Pathway*
glycine	GC/MS	**1.29**	0.0028	Glycine/serine/threonine metabolism
dimethylglycine	GC/MS	**1.80**	0.0219	Glycine/serine/threonine metabolism
N-acetylserine	GC/MS	**1.47**	0.0016	Glycine/serine/threonine metabolism
aspartate	GC/MS	**4.00**	0.0047	Alanine and aspartate metabolism
N-acetylhistidine	LC/MS neg	**1.18**	0.0259	Histidine metabolism
cadaverine	GC/MS	**4.76**	0.0018	Lysine metabolism
diaminopimelate	GC/MS	**2.76**	0.0008	Lysine metabolism
saccharopine	GC/MS	**3.21**	0.0002	Lysine metabolism
phenylacetate	LC/MS neg	**2.45**	0.0043	Phenylalanine & tyrosine metabolism
anthranilate	LC/MS pos	**6.67**	0.0001	Tryptophan metabolism
S-methylcysteine	GC/MS	**3.47**	0.0004	Cysteine/methionine/SAM/taurine
methionine sulfoxide	GC/MS	**4.13**	0.0029	Cysteine/methionine/SAM/taurine
S-adenosylhomocysteine (SAH)	LC/MS neg	**7.14**	0.0040	Cysteine/methionine/SAM/taurine
arginine	GC/MS	**1.20**	0.0185	Urea cycle;arginine/prolinemetabolism
trans-4-hydroxyproline	GC/MS	**1.64**	0.0263	Urea cycle;arginine/prolinemetabolism
glutathione, reduced (GSH)	LC/MS pos	**1.37**	0.0299	Glutathione metabolism
5-oxoproline	LC/MS neg	**1.75**	0.0048	Glutathione metabolism
glycylproline	LC/MS pos	**2.50**	0.0062	Dipeptide
pro-hydroxy-pro	LC/MS pos	**1.54**	0.0394	Dipeptide
phenylalanylalanine	LC/MS pos	**3.23**	0.0472	Dipeptide
valylasparagine	LC/MS neg	**2.57**	0.0025	Dipeptide
valylvaline	LC/MS neg	**2.69**	0.0254	Dipeptide
cyclo(gly-pro)	LC/MS pos	**5.26**	0.0161	Dipeptide
isoleucylglutamine	LC/MS neg	**3.17**	0.0004	Dipeptide
valyllysine	LC/MS neg	**1.86**	0.0211	Dipeptide
arginylmethionine	LC/MS pos	**2.44**	0.0442	Dipeptide
phenylalanylaspartate	LC/MS pos	**2.17**	0.0411	Dipeptide
tryptophylglutamate	LC/MS pos	**1.69**	0.0149	Dipeptide
glucosamine	GC/MS	**3.20**	0.0016	Aminosugars metabolism
N-acetylgalactosamine	GC/MS	**1.21**	0.0069	Aminosugars metabolism
N-acetylglucosamine 6-phosphate	GC/MS	**2.78**	0.0053	Aminosugars metabolism
fructose	GC/MS	**2.28**	0.0210	Fructose/mannose/galactose/starch
mannose	GC/MS	**1.75**	0.0124	Fructose/mannose/galactose/starch
mannose-6-phosphate	GC/MS	**1.47**	0.0104	Fructose/mannose/galactose/starch
trehalose	GC/MS	**3.23**	0.0408	Fructose/mannose/galactose/starch
maltotriose	GC/MS	**3.79**	0.0119	Fructose/mannose/galactose/starch
1,5-anhydroglucitol (1,5-AG)	GC/MS	**9.94**	0.0001	Fructose/mannose/galactose/starch
glycerate	GC/MS	**1.45**	0.0333	Fructose/mannose/galactose/starch
gluconate	GC/MS	**158.46**	0.0105	Nucleotide sugars, pentose metabolism

succinylcarnitine	LC/MS pos	**1.80**	0.0432	Krebs cycle
fumarate	GC/MS	**1.31**	0.0139	Krebs cycle
10-heptadecenoate (17:1n7)	LC/MS neg	**1.60**	0.0417	Long chain fatty acid
arachidonate (20:4n6)	LC/MS neg	**1.74**	0.0419	Long chain fatty acid
omega-3 arachidonic acid (20:4n3)	GC/MS	**1.59**	0.0146	Long chain fatty acid
n-butyl oleate	GC/MS	**1.45**	0.0468	Fatty acid, ester
oleoylethanolamide	LC/MS neg	**2.08**	0.0091	Endocannabinoid
cholate	LC/MS neg	**8.33**	0.0177	Bile acid metabolism
glycocholate	LC/MS pos	**8.33**	0.0033	Bile acid metabolism
taurocholate	LC/MS neg	**9.09**	0.0029	Bile acid metabolism
ethanolamine	GC/MS	**2.14**	0.0043	Glycerolipid metabolism
phosphoethanolamine	GC/MS	**1.33**	0.0080	Glycerolipid metabolism
glycerol 3-phosphate (G3P)	GC/MS	**1.96**	0.0073	Glycerolipid metabolism
glycerophosphorylcholine (GPC)	LC/MS pos	**3.03**	0.0028	Glycerolipid metabolism
1-palmitoylglycerophosphoethanolamine	LC/MS neg	**1.81**	0.0097	Lysolipid
1-stearoylglycerophosphoethanolamine	LC/MS neg	**1.36**	0.0452	Lysolipid
1-oleoylglycerophosphoethanolamine	LC/MS neg	**1.89**	0.0119	Lysolipid
1-palmitoleoylglycerophosphocholine*	LC/MS pos	**1.67**	0.0396	Lysolipid
1-stearoylglycerophosphocholine	LC/MS pos	**3.00**	0.0009	Lysolipid
inosine	LC/MS neg	**2.13**	0.0320	Purine metabolism, (hypo)xanthine/inosine containing
inosine 5'-monophosphate (IMP)	LC/MS pos	**2.44**	0.0097	Purine metabolism, (hypo)xanthine/inosine containing
adenosine-2',3'-cyclic monophosphate	LC/MS neg	**2.94**	0.0235	Purine metabolism, adenine containing
guanosine	LC/MS pos	**3.85**	0.0007	Purine metabolism, guanine containing
allantoin	GC/MS	**1.67**	0.0421	Purine metabolism, urate metabolism
cytidine	LC/MS pos	**1.77**	0.0035	Pyrimidine metabolism, cytidine containing
cytidine 5'-monophosphate (5'-CMP)	LC/MS pos	**1.47**	0.0010	Pyrimidine metabolism, cytidine containing
uridine	LC/MS neg	**5.26**	0.0025	Pyrimidine metabolism, uracil containing
uridine monophosphate (5' or 3')	LC/MS neg	**1.75**	0.0070	Pyrimidine metabolism, uracil containing
gulono-1,4-lactone	GC/MS	**1.83**	0.0141	Ascorbate and aldarate metabolism
pantothenate	LC/MS pos	**1.30**	0.0074	Pantothenate and CoA metabolism
benzoate	GC/MS	**4.41**	0.0005	Benzoate metabolism
anthraniloyl-O-glucose	LC/MS neg	**2.08**	0.0241	Benzoate metabolism

Significant increase in *lipl-4 Tg*

Significant decrease in *lipl-4 Tg*

References

1. C. Settembre, A. Fraldi, D. L. Medina, A. Ballabio, Signals from the lysosome: A control centre for cellular clearance and energy metabolism. *Nat. Rev. Mol. Cell Biol.* **14**, 283–296 (2013). Medline doi:10.1038/nrm3565

2. A. D. Patrick, B. D. Lake, Deficiency of an acid lipase in Wolman's disease. *Nature* **222**, 1067–1068 (1969). Medline doi:10.1038/2221067a0

3. M. C. Wang, E. J. O'Rourke, G. Ruvkun, Fat metabolism links germline stem cells and longevity in *C. elegans*. *Science* **322**, 957–960 (2008). Medline

4. M. Furuhashi, G. S. Hotamisligil, Fatty acid-binding proteins: Role in metabolic diseases and potential as drug targets. *Nat. Rev. Drug Discov.* **7**, 489–503 (2008). Medline

5. J. Storch, B. Corsico, The emerging functions and mechanisms of mammalian fatty acid-binding proteins. *Annu. Rev. Nutr.* **28**, 73–95 (2008). Medline

6. J. Goudeau, S. Bellemin, E. Toselli-Mollereau, M. Shamalnasab, Y. Chen, H. Aguilaniu, Fatty acid desaturation links germ cell loss to longevity through NHR-80/HNF4 in *C. elegans*. *PLOS Biol.* **9**, e1000599 (2011). Medline doi:10.1371/journal.pbio.1000599

7. C. Kenyon, J. Chang, E. Gensch, A. Rudner, R. Tabtiang, A *C. elegans* mutant that lives twice as long as wild type. *Nature* **366**, 461–464 (1993). Medline

8. S. Ogg, S. Paradis, S. Gottlieb, G. I. Patterson, L. Lee, H. A. Tissenbaum, G. Ruvkun, The Fork head transcription factor DAF-16 transduces insulin-like metabolic and longevity signals in *C. elegans*. *Nature* **389**, 994–999 (1997). Medline

9. S. H. Panowski, S. Wolff, H. Aguilaniu, J. Durieux, A. Dillin, PHA-4/Foxa mediates diet-restriction-induced longevity of *C. elegans*. *Nature* **447**, 550–555 (2007). Medline

10. P. P. Pathare, A. Lin, K. E. Bornfeldt, S. Taubert, M. R. Van Gilst, Coordinate regulation of lipid metabolism by novel nuclear receptor partnerships. *PLOS Genet.* **8**, e1002645 (2012). Medline

11. M. R. Van Gilst, H. Hadjivassiliou, A. Jolly, K. R. Yamamoto, Nuclear hormone receptor NHR-49 controls fat consumption and fatty acid composition in *C. elegans*. *PLOS Biol.* **3**, e53 (2005). Medline

12. B. N. Heestand, Y. Shen, W. Liu, D. B. Magner, N. Storm, C. Meharg, B. Habermann, A. Antebi, Dietary restriction induced longevity is mediated by nuclear receptor NHR-62 in *Caenorhabditis elegans*. *PLOS Genet.* **9**, e1003651 (2013). Medline

13. B. Lakowski, S. Hekimi, The genetics of caloric restriction in *Caenorhabditis elegans*. *Proc. Natl. Acad. Sci. U.S.A.* **95**, 13091–13096 (1998). Medline doi:10.1073/pnas.95.22.13091

14. G. Astarita, B. Di Giacomo, S. Gaetani, F. Oveisi, T. R. Compton, S. Rivara, G. Tarzia, M. Mor, D. Piomelli, Pharmacological characterization of hydrolysis-resistant analogs of oleoylethanolamide with potent anorexiant properties. *J. Pharmacol. Exp. Ther.* **318**, 563–570 (2006). Medline doi:10.1124/jpet.106.105221

15. J. Fu, G. Astarita, S. Gaetani, J. Kim, B. F. Cravatt, K. Mackie, D. Piomelli, Food intake regulates oleoylethanolamide formation and degradation in the proximal small intestine. *J. Biol. Chem.* **282**, 1518–1528 (2007). Medline doi:10.1074/jbc.M607809200

16. M. Lucanic, J. M. Held, M. C. Vantipalli, I. M. Klang, J. B. Graham, B. W. Gibson, G. J. Lithgow, M. S. Gill, *N*-Acylethanolamine signalling mediates the effect of diet on lifespan in *Caenorhabditis elegans*. *Nature* **473**, 226–229 (2011). Medline doi:10.1038/nature10007

17. J. Fu, S. Gaetani, F. Oveisi, J. Lo Verme, A. Serrano, F. Rodríguez De Fonseca, A. Rosengarth, H. Luecke, B. Di Giacomo, G. Tarzia, D. Piomelli, Oleylethanolamide regulates feeding and body weight through activation of the nuclear receptor PPAR-alpha. *Nature* **425**, 90–93 (2003). Medline doi:10.1038/nature01921

18. G. Hadwiger, S. Dour, S. Arur, P. Fox, M. L. Nonet, A monoclonal antibody toolkit for *C. elegans*. *PLOS ONE* **5**, e10161 (2010). Medline doi:10.1371/journal.pone.0010161

19. M. Merkel, A. C. Tilkorn, H. Greten, D. Ameis, Lysosomal acid lipase. Assay and purification. *Methods Mol. Biol.* **109**, 95–107 (1999). Medline

20. G. Haemmerle, A. Lass, R. Zimmermann, G. Gorkiewicz, C. Meyer, J. Rozman, G. Heldmaier, R. Maier, C. Theussl, S. Eder, D. Kratky, E. F. Wagner, M. Klingenspor, G. Hoefler, R. Zechner, Defective lipolysis and altered energy metabolism in mice lacking adipose triglyceride lipase. *Science* **312**, 734–737 (2006). Medline doi:10.1126/science.1123965

21. A. M. Evans, C. D. DeHaven, T. Barrett, M. Mitchell, E. Milgram, Integrated, nontargeted ultrahigh performance liquid chromatography/electrospray ionization tandem mass spectrometry platform for the identification and relative quantification of the small-molecule complement of biological systems. *Anal. Chem.* **81**, 6656–6667 (2009). Medline

22. C. D. Kane, D. A. Bernlohr, A simple assay for intracellular lipid-binding proteins using displacement of 1-anilinonaphthalene 8-sulfonic acid. *Anal. Biochem.* **233**, 197–204 (1996). Medline

23. G. J. Hermann, L. K. Schroeder, C. A. Hieb, A. M. Kershner, B. M. Rabbitts, P. Fonarev, B. D. Grant, J. R. Priess, Genetic analysis of lysosomal trafficking in *Caenorhabditis elegans*. *Mol. Biol. Cell* **16**, 3273–3288 (2005). Medline doi:10.1091/mbc.E05-01-0060